Article

Load Frequency Control in Two-Area Multi-Source Power System Using Bald Eagle-Sparrow Search Optimization Tuned PID Controller

T. Dharma Raj [1], C. Kumar [2] , Panos Kotsampopoulos [3],* and Hady H. Fayek [4]

[1] The Department of Electrical and Electronics Engineering, V V College of Engineering, Tirunelveli 627657, India
[2] The Department of Electrical and Electronics Engineering, M.Kumarasamy College of Engineering, Karur 639113, India
[3] School of Electrical and Computer Engineering, National Technical University of Athens, 15773 Athens, Greece
[4] Electromechanics Engineering Department, Faculty of Engineering, Heliopolis University, Cairo 11785, Egypt
* Correspondence: kotsa@power.ece.ntua.gr

Abstract: For power system engineers, automated load frequency control (LFC) for multi-area power networks has proven a difficult problem. With the addition of numerous power generation sources, the complexity of these duties becomes even more difficult. The dynamic nature of linked power networks with varied generating sources, such as gas, thermal, and hydropower plants, is compared in this research. For the study to be more accurate, frequency and tie-line power measurements are used. For precise tuning of proportional-integral-derivative (PID) controller gains, the Bald Eagle Sparrow search optimization (BESSO) technique was used. The BESSO algorithm was created by combining the characteristics of sparrows and bald eagles. The performance of BESSO is determined by comparing its findings to those acquired using traditional approaches. In terms of Integral Time Absolute Error (ITAE), which is the most important criterion used to reduce system error, the findings presented in this study indicate the effectiveness of the BESSO-PID controller. Finally, sensitivity analysis and stability analysis proved the robustness of the developed controller. The settling times associated with the tie-line power flow, frequency variation in area-1, and frequency variation in area-2, respectively, were 10.4767 s, 8.5572 s, and 11.4364 s, which were all less than the traditional approaches. As a result, the suggested method outperformed the other strategies.

Keywords: LFC; multiple source power system; PID controller; ITAE; optimization

1. Introduction

Electricity is unquestionably regarded as a potentially clean and vital source of energy in today's world. An interconnected power system includes generation, transmission, distribution, and loads. Multiple geographically placed service regions are connected by a tie-line in an enlarged interconnected power system. As a result, any unanticipated load disturbance in one of the regions would result in unwanted modifications in the tie-line power and frequency in other locations [1,2].

To maintain the scheduled power exchange with multiple areas, the generation inside each area should be managed. Load frequency control (LFC) is a principal operator in the Automatic Generation Control (AGC) domain due to its enhanced ability to control power [3]. Due to their uneven distribution and lack of renewability, non-renewable resources raise questions regarding their availability for current and future generations [4]. Lithium-ion Batteries (LiBs) are becoming more prevalent in both commercially accessible equipment and research activities for energy storage [5]. One of the primary drivers of the growth and adoption of microgrid applications is energy security [6]. The frequency of a

power system and its variation are related to active power demands. When the consumed active power is more than the generated active power, the system frequency oscillates and falls short of the target value. LFC is used to solve this problem by regulating the produced power and maintaining the nominal frequency at its set measure [2]. LFC is a significant power system component that aims to achieve two goals: preserving the system's frequency and keeping tie-line power variation below specified levels.

Frequency is an essential stability criterion in a system considering two or more areas. As a result, the frequency must be maintained invariably based on the balance of active power to give superior stability [3]. Furthermore, using LFC prevents grid instability that may be produced by disturbances [2]. LFC's control goal is to maintain the variation in frequency and the overall tie-line flow deviation among the control zones as low as possible. In particular, the LFC should maintain stability in the face of nonlinearities in the system, model parameter errors, and resonance attacks [7] that may arise in real power systems. A lot of effort has been invested into creating control solutions for the issues associated with LFC, and they are divided into two types.

In the first type, innovative controllers have been designed using different advanced methodologies [8]. Model predictive control [9], H∞ and μ-synthesis [10], fuzzy logic [11], and the sliding model approach [12] are used to solve the LFC problem. The PID [13] or PI controller [14] is the secondary category, which is the engineer's favored option due to its basic yet dependable control structure. In addition, the PI/PID controller requires fewer user skills and has a simpler dynamic model, making it more practical in engineering practice [15].

To attenuate the fluctuations of the power system's frequency, traditional PID controller methods, namely the Ziegler Nichols method, the Cohen-Coon method, etc., were utilized [16]. Traditional method-based controllers, however, are ineffective for complex power system networks. Because of their capacity to manage errors and disturbances, various efforts to employ optimization methodologies to optimize the parameters have been recently prepared [17–19].

Many schemes of control based on soft computing methodologies have been devised in recent decades to uphold the frequency and tie-line power at nominal measures. The BFO, GA [20], TLBO Algorithm [21], and GWO [22] are examples of these control systems. These controllers not only keep the system's frequency stable, but they also keep the power system's steady state errors to a minimum [23]. These approaches have various merits, including being simple to apply and having a faster convergence speed. It also has several flaws, such as precociousness, excellent procedural reliability, and parametric flexibility [3]. Wind energy, which is obtained by wind turbines, is one of the most extensively used and affordable renewable energy sources [24].

This study's major goal is to provide a strategy for autonomous load frequency control in a two-area power system with various sources. Multiple sources, such as hydropower plants, gas turbine power plants, and thermal power plants, make up the two-area power system. The research's significance relies on the best tuning of PID controller constraints using the proposed bald eagle-sparrow search optimization algorithm, which mimics bald eagles' hunting style or clever social behavior when searching for seafood, as well as the anti-predation actions and collective wisdom foraging of sparrow search agents. To verify that the constraints were within acceptable limits, the PID controller settings were modified by minimizing the ITAE measurement through the proposed BESSO algorithm. The findings showed that the proposed new approach was successful in optimizing the settings of a PID controller.

The major contributions of the paper are:

- A novel optimized PID controller is proposed to reduce tie-line power and frequency oscillations induced by load disturbances. BESSO was introduced to estimate the most favorable parameters of the PID controller.
- The proposed BESSO algorithm follows the hunting style of bald eagles in searching for food and also the anti-predation actions and collective wisdom foraging of sparrows.

- To show BESSO's supremacy in LFC, exhaustive comparative research with various newly reported LFC techniques was conducted.
- The performance of test systems was investigated with repeated load variations to confirm the proposed controller's stability. Finally, a statistical analysis was conducted to confirm the BESSO technique's robust behavior in LFC.

The structure of the manuscript is arranged as follows. Section 2 provides a review of research publications related to the requirement to manage LFC and tie-line power. The proposed method of load frequency regulation is described in Section 3. Subsequently, the results obtained are discussed in Section 4. Finally, in Section 5, the conclusions of the paper are presented.

2. Literature Survey

A literature review of the existing models of LFC and the control of tie-line power follows:

Dipayan Guha et al. [25] attempted to apply the whale optimization algorithm (WOA) for discovering the most favorable and realistic solutions to LFC issues in power systems. The optimization strategy was independently utilized for tuning controller parameters. However, the concurrent reduction of settling time was not achievable, and hence, some compromises were justified in the results.

Reza Mohammadikia and Mortaza Aliasghary [2] designed a fractional order fuzzy PID (FOFPID) controller for load frequency control. Here, the BBO algorithm was used for tuning the controller parameters. However, the integral term demonstrated poor performance concerning steady-state variation in frequency and oscillation.

Kangdi Lu et al. [15] introduced a PI controller modeled by limited population extreme optimization for LFC of multi-area systems. Three dissimilar two-area power systems were considered as test models to reveal the efficacy of the developed controller. However, the non-linear terms were not taken into consideration in the state space model, which was found to be the limitation of the model.

Yasser Ahmed Dahab et al. [19] introduced an adaptive LFC strategy for power systems based on the regulation of the parameters of the integral controller through ESO. However, the objective of the system was formulated based on the transfer function of the power plant with the consideration of no load disturbance. This may lead to poor performance during disturbances in load and changes in system parameters.

Dipayan Guha et al. [26] explained the SSA-optimized cascaded tilt–integral–derivative controller (CC-TID) for LFC control. The suggested controller incorporated the advantages of the cascade control method as well as fractional-order mathematics. The suggested model employed a TID controller as the slave controller and a PI controller as the master controller. The presented technique outperformed the comparison methods concerning converging power density, profile, and statistical findings when compared to differential evolution and flower pollination algorithms.

Mohamed Barakat et al. [27] provided a well-organized conjunction of the WCA with a cascade tilt-derivative tilt-integral (TD-TI) cascade controller. The model was implemented under different standpoints to validate the suggested system's effectiveness. An important addition to the investigated controller was that it preserved stable operation in both scenarios with and without HVDC connections when substantial load variations were investigated.

Krishan Arora et al. [28] developed a technique based on HHO to resolve the issues associated with frequency-associated problems. The strategy was analyzed under various regular benchmark functions to handle various optimization problems.

Rajiv Kumar and Sharma [3] tested the whale optimization algorithm (WOA)-based controller for the evaluation of design, stability administration, and investigation of the performance of a two-area multi-power system. The model adjusted well with various working states of load agreements, but it was unsuccessful in tuning the power of the multi-area system. This method's LFC, however, had a poor system frequency range. Although it

had a faster computing rate, the quality of the system was overestimated. However, it had difficulty determining the best settings [6].

Nian Wang et al. [29] designed a strategy based on IWFOA to handle models with highly non-linear constraints. The outcomes showed that the control model could attain the targets of the control system and completely use the different features of each generator. However, the frequency of the controller could not attain the anticipated target in control due to the effect of different non-linear parameters.

Deepak Kumar Gupta et al. [30] presented a novel optimization strategy to attain the goal of automatic LFC. In particular, the optimization strategy controlled the change in frequency of a power system with multiple sources. The outcomes attained were, however, not the best possible, and the strategy also ended up with a slow convergence.

Debasis Tripathy et al. [31] compared the dynamic response of an FLC-based PID with various membership functions for LFC in a two-area power system. The SMO algorithm was used to optimize the controller settings. The suggested algorithm's superiority was demonstrated by comparing the results to those of commonly used algorithms, such as PSO and TLBO. The key benefits of this method were that it balanced both exploitation and exploration of search space, while also addressing the issues of early completion and stagnation.

Mohamed Abdul Raouf Shafei et al. [32] intended FLC to act as the primary LFC. FLC's evolving performance was improved by enhancing its constraints for various cost functions through PSO. One or two FLCs would be inserted into the PV model to operate as an output controller, as an alternative to MPPT, to increase the overall efficiency of the system. To boost dependability, RFB was introduced in the conceptual scheme as a frequency stabilizer. RFB offers a deep discharge capability of up to 90% with a potentially infinite number of power levels and a quick time reaction for extreme load fluctuations.

In a study by Ali et al. [33], a proportional-integral proportional-derivative (PI-PD) controller based on a dandelion optimizer (DO) was examined for a realistic multi-area, multi-source, realistic IPS with nonlinearities. In a two-area network with a 10% step load perturbation, the output responses of the DO-based PI-PD were compared with the hybrid approach using the artificial electric field-based fuzzy PID algorithm (HAEFA), the Archimedes optimization algorithm (AOA), learning performance-based behavior optimization (LPBO), and modified particle swarm optimization (MPSO)-based PI-PD control schemes (SLP).

In a study by Kumar et al. [34], the automatic generation control (AGC) of inter-connected multi-source (thermal-hydro-gas) multi-area deregulated power systems was addressed, using a novel improved gravitational search algorithm-binary particle swarm optimization (IGSA-BPSO)-driven proportional-integral-derivative (PID) controller. With GSA and PSO-driven PID controllers, the effectiveness and robustness of the proposed controller were compared and examined. The findings from simulations and mathematical formulations demonstrated that the suggested IGSA-BPSO-driven PID controller was superior to the other two approaches in terms of settling time, overshoot, and convergence time.

Research Gap

The author in [35] presented a novel cascade controller for the AGC of a hybrid power supply system. The method was mostly used in one to three areas and a PEV system. The author in [36] used a PID controller to create a TCSC-incorporated damping strategy that followed the AGC. They developed particle swarm optimization (PSO) as an enhanced optimization approach based on the chaotic constraint and the crossover operator, which was utilized to find the best outcome. It did, however, need more active performances [3]. After the process of deregulation, the authors in [37] presented the DMPC of a distributed multi-area power system. The researchers concentrated on LFC difficulties in the context of a deregulated sector of energy. The authors in [38] developed a tilt-integrated controller to perform the LFC of a two-area power system, which possessed a higher performance and was more reliable. The above limitations acted as the motivation for the development of

the proposed strategy that, in turn, assisted in enhancing the load frequency control in the two-area multi-source power system, overcoming the challenges.

3. Proposed Strategy of LFC in a Two-Area Power System

Residential, industrial, and commercial sectors are all becoming increasingly reliant on power. Renewable energy integration is a superior option since it reduces dependence. The customary conditions of electricity system functioning can be changed via deregulation. As a result, two-area power systems with distributed generation have attracted a lot of attention. To fulfill excessive load requirements, the recent power system primarily consists of multiple control zones with varying sources of generation with non-identical capabilities.

Any disparity between supply and demand causes area frequency to deviate from a predetermined level, resulting in unintended power-sharing with surrounding control areas. Previously, the frequency variation following load disturbances was controlled via a fly-ball mechanism. Because of the massive variations in the structure of power systems, the inclusion of new nonlinearities and limitations, and the large load demand, the fly-ball strategy is not suitable for handling frequency fluctuation. As a result, finding and implementing a supplemental control method to alleviate this problem is understood, and is carried out by LFC [2].

LFC continually monitors the difference between generation and load demand and controls steam flow through the turbine by adjusting the governor valve position. The successful operation of the LFC is strongly dependent on the choice of the controller parameters; an incorrect choice may result in power system instability. This is achieved in this paper by using the proposed BESSO algorithm for the optimal tuning of PID parameters. LFC overcomes the problems in the AGC by acting as a level control.

The AGC model used for the study is a multi-source equivalent two-area power system. Each region in the model has a thermal unit, a gas unit, and a hydro unit. The two locations are linked by a tie line, which permits electric power to be transferred between the interlinked sectors. The control unit checks the tie-line power and frequency variations and attempts to return the system to normal operation under unfavorable situations, such as major load disturbances.

3.1. Dynamic Model

Most of the electricity areas are linked to their surrounding territories, making load frequency control a challenge. This section deals with the modeling of a traditional interconnected power system of multiple areas, in which each region is modeled by four key elements: a generator, a turbine, a governor, and a load. A tie-line connects each section of this integrated electrical power system network to the others. In the presence of a PID controller, the LFC loop is placed in every control zone to regulate the tie-line power and load frequency. The proposed BESSO approach is designed for fine-tuning PID controller settings.

3.1.1. Generator Modeling

The generator is a device that turns the turbine's mechanical energy into electrical energy. The swing formula of a synchronous generator to only disturbance expresses the relationship between electrical and mechanical power as follows,

$$M\frac{d\Delta r}{dt} = \Delta P_m - \Delta P_e \tag{1}$$

where, M indicates the inertia constant, Δr represents the deviation in rotor speed, ΔP_e is the change in electrical power, and ΔP_m is the variation in mechanical power. The load in a power system is made up of many sorts of electrical components that may or may not

be affected by frequency changes [30]. The following is the formula for the electric power relationship based on frequency change, which is formulated as,

$$\Delta P_e = \Delta P_D + D\Delta r \tag{2}$$

where D is the load damping constant, ΔP_D indicates the non-frequency sensitive load variation, and $D\Delta r$ indicates the frequency sensitive load variation. In a multi-machine system with three power-producing units working in parallel in the same territory, such as a hydropower system, a thermal power system, and a gas-turbine power system, an equivalent generator is constructed to indicate the entire area for simplicity [39,40]. The equivalent load-damping constant, as well as the corresponding generator inertia constant, are written as,

$$D_{eq} = \sum_{i=1}^{n} D_i \tag{3}$$

$$M_{eq} = \sum_{i=1}^{n} M_i \tag{4}$$

The expression for the equivalent generator is expressed as,

$$\frac{d\Delta f_i}{dt} = \frac{1}{M_{eq_i}} \left(\sum_{l=1}^{n} \Delta P_{Tli} - \sum \Delta P_{tie_i} - \Delta P_{D_i} - D_{eq_i} * \Delta f_i \right) \tag{5}$$

where, $i = \{1, 2, 3\}$ indicates the power-producing units, namely a hydropower system, a gas-turbine power system, and a thermal power system [41].

3.1.2. Tie-Line Modeling

In the power systems of multiple areas with interconnections, some regions are connected to each other via tie lines, and the power is transferred among these areas through such tie lines [42].

The tie-line concept is represented in block diagram form in Figure 1 [41]. Consider, the tie-line power transfer from area i to area j, and the variation ΔP_{Tij} from the nominal flow is written as,

$$\Delta P_{Tij} = \frac{T}{s} \left(\Delta \omega_i - \Delta \omega_j \right) \tag{6}$$
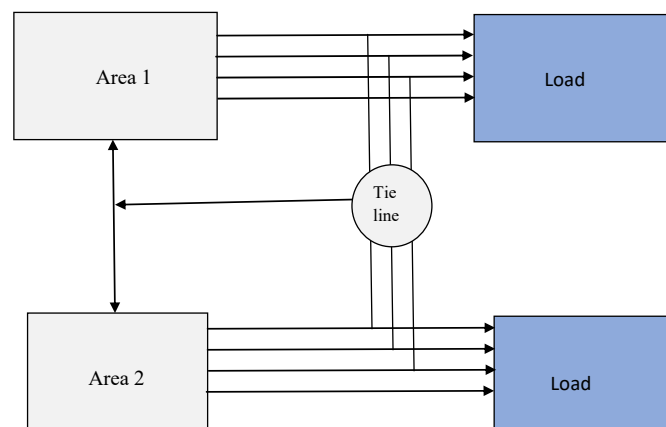

Figure 1. Schematic representation of the tie-line model.

3.1.3. LFC Modeling

The LFC loop's main goal is to establish the governor units' outputs and manage their reference operating point. According to the independent system operator (ISO), the frequency and total exchange of power flow are assessed to estimate the control area [41,43]. The following is the formula for the area control error,

$$ACE_i = B_i\Delta f_i + \Delta P_{Tij} \tag{7}$$

In the case of a two-area power system, the frequency bias coefficients B_1 and B_2 are given by,

$$B_1 = \frac{1}{R_1} + D_1 \tag{8}$$

$$B_1 = \frac{1}{R_1} + D_2 \tag{9}$$

The area control errors ACE_1 and ACE_2 are,

$$ACE_1 = B_1\Delta f_1 + \Delta P_{tie1} \tag{10}$$

$$ACE_2 = B_2\Delta f_2 + \Delta P_{tie2} \tag{11}$$

where $\Delta P_{tie1,2}$ is the error of the tie-line power transfer from area 1 to area 2. The term B_i is the frequency response characteristics for area i.

In general, the equivalent frequency bias factor is expressed as,

$$\beta_{eq} = \sum_{i=1}^{n} \frac{1}{R_i} + \sum_{i=1}^{n} D_i \tag{12}$$

To maintain the power system as secure, the tie-line power flow and the frequency must be controlled. In other words, instabilities caused by changes in source powers, such as hydro, thermal, and gas-turbine power plants and loads, must be reduced. Each generator is connected to a PID controller to perform the power balance and maintain system frequency at the pre-defined levels.

3.2. Description of PID Controller

A controller's main goal is to find a suitable combination of controls that always allow the system to attain the desired state with minimal deviations. Because the equations for a controlled system in the general case are complicated, the controller must be able to include stochastic effects and non-linear features in its design. PID controllers, which have enhanced characteristics and well-established design methodologies, are one of the most frequent industrial controllers [44]. Figure 2 shows the basic PID control arrangement. The system becomes more stable as a result of the proportional controller's assistance in lowering the steady-state error. These controllers can make the over-damped system's slow response time faster.
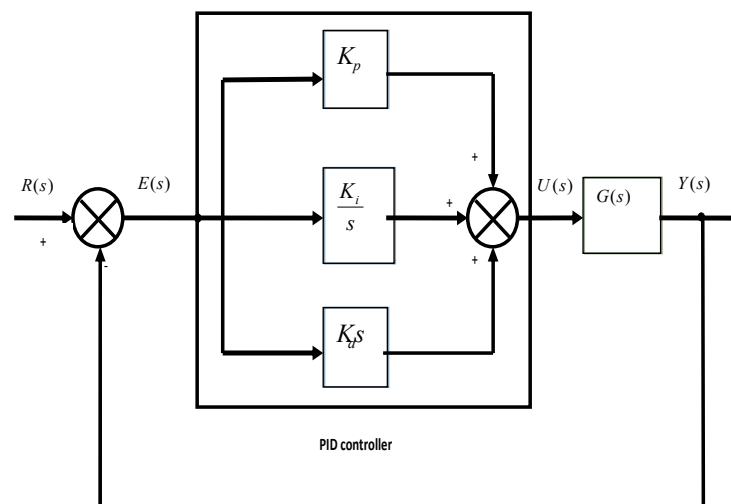

Figure 2. Block diagram of PID controller.

The output expression of the PID controller is,

$$u(t) = K_p e_p(t) + K_i \int_0^t e_i(t)dt + K_d \frac{de_d(t)}{dt} \tag{13}$$

where, K_p, K_i, K_d correspondingly indicate the proportional constant, integral constant, and derivative constant. The term $u(t) = K_p e_p(t)$ with the hypothesis that $K_i = K_d = 0$ shows that the control is proportionate to the error at any given moment and is a function of the current error value. When the error is significant, so is the control signal. When the system noticeably deviates from the objective, the control makes no adjustments to bring it back to its initial state.

As a result, the integral term appears, which is written as, $u(t) = K_i \int_0^t e_i(t)dt$ with the consideration that $K_p = K_d = 0$. With the inclusion of this integral, the system is guaranteed to have zero steady-state errors to a step input. When the term is non-zero, the control signal becomes more and stronger as time passes. This causes the plant to react if the plant's output begins to change. In summary, the integral term is determined to be the accumulator of previous error measurements. To increase the system performance, the derivative term $u(t) = K_d \frac{de_d(t)}{dt}$ is inserted with the assumption that $K_p = K_i = 0$.

The derivative term describes how the rate of change in error affects system control. As a result, the derivative term is determined by future error values. In setting its control value, the PID controller takes into account past, present, and future errors. To sustain the target frequency of the system and reduce power fluctuations, the suggested PID controller model employs a secondary control approach known as AGC, which includes tie-line power flow regulation. AGC is generally used for raising or lowering the generator power outputs in two-area power systems.

3.2.1. Automatic Generation Control

The proper tuning of PID parameters is required for the improved operation of the power system under various operating modes. The model's uncertainty and dynamic fluctuations are intended to be addressed by fine-tuning the PID controller's settings. The power system must be extremely sensitive to load fluctuation variations and maintain the predicted point for all parameters [45]. ITAE is determined to be the one that provides good results for parametric optimization concerning overshoot and settling time, out of a variety of performance indices that measure the efficacy of power systems [30]. Accordingly, ITAE is regarded as the objective function to be reduced in the proposed study, and the expression of ITAE in a two-area power system is expressed as,

$$ITAE = \int_0^t (|\Delta f_1| + |\Delta f_2| + |\Delta P_{tie}|) \cdot t \cdot dt \tag{14}$$

where ΔP_{tie} is the variation in tie-line power, Δf_1 indicates the variation in frequency corresponding to area 1, and Δf_2 represents the variation in frequency corresponding to area 2. The proposed BESSO optimization approach for determining the PID controller parameters minimizes the objective function ITAE.

The constraints to be maintained are,

$$\left. \begin{array}{l} K_{p\min} < K_p < K_{p\max} \\ K_{i\min} < K_i < K_{i\max} \\ K_{d\min} < K_d < K_{d\max} \end{array} \right\} \tag{15}$$

Furthermore, for a two-area power system, the differential equation of a PID controller becomes,

$$u_1 = K_{p1} \cdot ACE_1 + K_{i1} \int ACE_1 + K_{d1} \frac{dACE_1}{dt} \qquad (16)$$

$$u_2 = K_{p2} \cdot ACE_2 + K_{i2} \int ACE_2 + K_{d2} \frac{dACE_2}{dt} \qquad (17)$$

For the proposed model, it is obvious from Equations (11) and (12) that ACE is dependent on frequency change and the power through the tie-line. With ACE as the input to the PID controller, the parameters of which are optimally tuned via the suggested BESSO algorithm to regulate the deviation in tie-line power and frequency. Figure 3 shows the Simulink implementation of the proposed two-area power system.
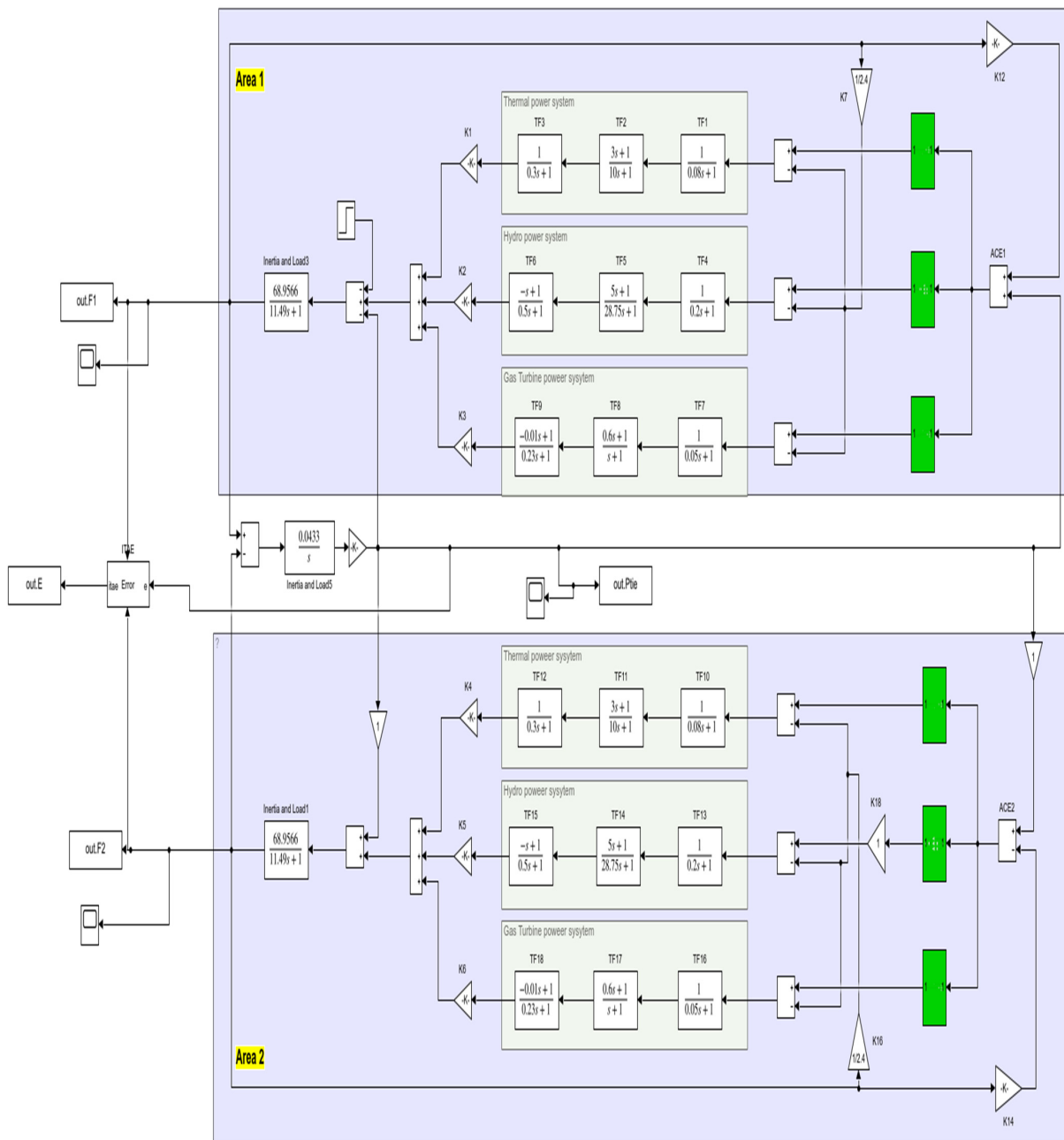

Figure 3. Simulink execution of the proposed model.

3.2.2. Overview of Proposed BESSO Algorithm

The proposed work presents a heuristic-based new hybrid optimization technique for automatic LFC of two-area multiple-source power systems. The proposed intelligent strategy makes use of the main features of two different optimization strategies, such as the BaEO and the SpSOA. This hybrid technique is used for the parametric tuning of the PID to normalize the fluctuations in power systems. The PID is one of the most widely used controllers and is ubiquitous in today's modern industries. Moreover, it is widely applicable in systems with single-input and single-output systems. The majority of typical optimization methods have features centered on the organisms' food-seeking tendencies, implying a dynamic nature in dealing with convergence difficulties. The dynamic properties linked with the traits of bald eagles and sparrows are used in the proposed BESSO method to tackle the convergence issue.

In other words, the capacity of sparrows to defend themselves against predators is inherited from the fearless nature of bald eagles while attacking prey [46]. When opposed to single optimization techniques, which often result in local optimum solutions, this improves the algorithm's capacity to obtain the global optimal solution with a higher convergence rate. In comparison to previous approaches, the proposed BESSO algorithm has a lower computational cost. The BESSO algorithm's operating concept consists of three key phases of operations: selection, search, and prey. These steps are critical for obtaining consistently good results and identifying an all-around ideal solution. In terms of the objective ITAE, the proposed BESSO algorithm beats existing solutions. The necessary parameters of the BESSO algorithm are first defined, and then the training and test phases are executed. The fitness function is then configured, and each search agent's fitness measure is determined. The optimal parameters are found by applying the BESSO method to optimize the PID controller's settings. The algorithmic procedure of the proposed BESSO algorithm is explained below,

Step 1: Objective function: The proposed BESSO method aims to reduce the ITAE measurement to the smallest possible value. The PID settings are fine-tuned by minimizing the objective function. The proposed optimization problem's objective is expressed as, Min (ITAE).

Step 2: Parameter and Population initialization: The parameters and the numbers of bald eagles are initialized in the next step. In addition, the maximum number of iterations is initialized. Each bald eagle takes a position vector indicating the current position as,

$$E_a = (E_1, E_2, \ldots, E_k); \qquad (a = 1, 2, \ldots, j, \ldots, p) \tag{18}$$

where E_a indicates the total bald eagles in the search space that varies from $1, 2, \ldots, p$ and E_j is the jth search agent. The fitness of each bald eagle is stored as,

$$R_a = (R_1, R_2, .., R_p) \tag{19}$$

Each bald eagle's fitness values are kept in the form of the above expression, which aids in determining the survival of the fittest throughout the whole population.

Step 3: Update of Position: The bald eagles' location may be updated using three different operations, such as the selection phase, the searching phase, and the phase of prey.

Phase 1: Selection phase: The bald eagles choose the search area at random and then evaluate the prey to choose the optimal location. At this step, the leader bald eagle's position is mostly assessed using a priori knowledge and location-changing characteristics, which are stated as,

$$E_q^{s+1} = E_{best} + \alpha \cdot \beta \cdot \left(E_{mean} - E_q^s \right) \tag{20}$$

where, E_q^{s+1} is the location of the qth bald eagle search agent at $(s+1)^{th}$ iteration. α represents the control constraint for variation in location changing from 1.5 to 2, β is the random variable that changes inside the limit $[0, 1]$, E_{best} is the best-ever location attained

by the bald eagles, E_{mean} signifies that the eagle search agents use all of the information from previous placements.

Phase 2: Searching phase: The spiral movement of the bald eagles improves the pace of the search and determines the best dive capture position. Based on this operation, the bald eagle search agents' position is described as,

$$E_q^{s+1} = E_q^s + c(q) \cdot \left(E_q^s - E_{mean} \right) + g(q) \cdot \left(E_q^s - E_q^{s-1} \right) \tag{21}$$

$$c(q) = \frac{ck(q)}{\max(|ck|)} \text{ and } g(q) = \frac{gk(q)}{\max(|gk|)} \tag{22}$$

$$ck(q) = k(q) \cdot \sin \theta(q) \text{ and } gk(q) = k(q) \cdot \cos \theta(q) \tag{23}$$

$$k(q) = \theta(q) + N \cdot Rand \tag{24}$$

$$\theta(q) = h \cdot \Pi \cdot Rand \tag{25}$$

where $\theta(q)$ is the polar angle of the spiral equation and $k(q)$ is the polar thickness of spiral formulation, N indicates a parameter that concludes the searching cycles and lies between 0.5 and 2, *Rand* is a random variable that changes from 0 to 1, and $c(q)$ and $g(q)$ are the polar coordinates of the bald eagles.

Phase 3: Phase of Prey: The bald eagle search agents dive fast from the most excellent position in the search area towards the target prey, and the rest of the search agents follow suit and attacks them. At this point in the procedure, the situation is stated as follows,

$$E_{q,bald}^{s+1} = Rand \cdot E_{best} + c_1(q) \cdot \left(E_q^s - b_1 \cdot E_{mean} \right) + g_1(q) \cdot \left(E_q^s - b_2 \cdot E_{best} \right) \tag{26}$$

$$c_1(q) = \frac{ck(q)}{\max(|ck|)} \text{ and } g_1(q) = \frac{gk(q)}{\max(|gk|)} \tag{27}$$

$$ck(q) = k(q) \cdot \sin \theta(q) \text{ and } gk(q) = k(q) \cdot \cos \theta(q) \tag{28}$$

$$k(q) = \theta(q) \tag{29}$$

$$\theta(q) = h \cdot \Pi \cdot Rand \tag{30}$$

where, b_1 and b_2 are the intensity of exercise in bald eagles to the best and center location, and holding the measure in the range [1, 2]. The sluggish pace of convergence and the danger of becoming caught in the local optimal solution are the algorithm's key limitations, despite the fact that this technique only requires a few parameters to be set. As a result, the features of bald eagles are inherited together with those of sparrows, resulting in a faster rate of convergence and a worldwide optimum solution. The versatility of sparrow traits in engineering sectors [47] is one of the reasons for their adoption. The ability to defend against predators is a key property of sparrows, and it is inherited from the features of bald eagles in the suggested technique. The sparrows' location can be adjusted as follows:

$$E_q^{s+1} = E_{best}^s + \varepsilon \left| E_q^s - E_{best}^s \right| \tag{31}$$

$$E_{q,sparrow}^{s+1} = E_{best}^s (1 - \varepsilon) + \varepsilon E_q^s \tag{32}$$

where ε is the control parameter associated with step size, $E_{q,sparrow}^{s+1}$ is the location of the sparrow at $(s+1)^{th}$ iteration, E_{best}^s is the current global optimum location of the sparrow. Finally, the hybrid sparrow and bald eagle's position is established as follows, based on the traits of the sparrow and the bald eagle, with equal consideration given to both features,

$$E_q^{s+1} = 0.5 E_{q,bald}^{s+1} + 0.5 E_{q,sparrow}^{s+1} \tag{33}$$

$$E_q^{s+1} = 0.5\left[Rand \cdot E_{best} + c_1(q) \cdot \left(E_q^s - b_1 \cdot E_{mean}\right) + g_1(q) \cdot \left(E_q^s - b_2 \cdot E_{best}\right)\right] + 0.5\left[E_{best}^s(1-\varepsilon) + \varepsilon E_q^s\right] \tag{34}$$

$$E_q^{s+1} = \frac{1}{2}\left\{\left[Rand \cdot E_{best} + c_1(q) \cdot \left(E_q^s - b_1 \cdot E_{mean}\right) + g_1(q) \cdot \left(E_q^s - b_2 \cdot E_{best}\right)\right] + \left[E_{best}^s(1-\varepsilon) + \varepsilon E_q^s\right]\right\} \tag{35}$$

Step 4: Arrangement of solutions: The bald eagles are ordered according to their fitness measurements, with solutions with lower fitness levels being ignored. The present solution is replaced with the one that has the best fitness measure. Otherwise, the old solution continues to be the best option.

Step 5: Termination: The method is finished when the maximum number of iterations has been completed and the best solution has been found. Table 1 shows the pseudocode of the proposed BESSO optimization algorithm. Figure 4 shows the flowchart of the proposed model.

Table 1. Pseudocode of BESSO optimization algorithm.

| Sl. No.	Pseudocode of BESSO Algorithm
1	**Start**
2	**Input:** $E_a = (E_1, E_2, \dots, E_k);$ $(a = 1, 2, \dots, j, \dots, p)$
3	**Output:** E_q^{s+1}
4	Initialize the population of search agents
5	Initialize parameters
6	Initialize maximum iteration
7	For each search agent
8	{
9	*Phase 1: Selection phase:*
10	Update the new solution based on Equation (19)
11	*Phase 2: Searching phase:*
12	Update the new solution based on Equation (20)
13	*Phase 2: Phase of Prey:*
14	Update the new solution based on Equation (35)
15	Evaluate fitness measures for each solution
16	Arrange the solutions based on a fitness measure
17	Re-evaluate the fitness measure
18	**If**
19	{
20	$R_{a,old} < R_{a,new}$
21	Replace the old solution with the new solution
22	**Else**
23	Consider the old solution as the best solution
24	**End If**
25	}
26	}
27	Update position of search agents based on fitness
28	**Stop**
29	**Output** E_q^{s+1}
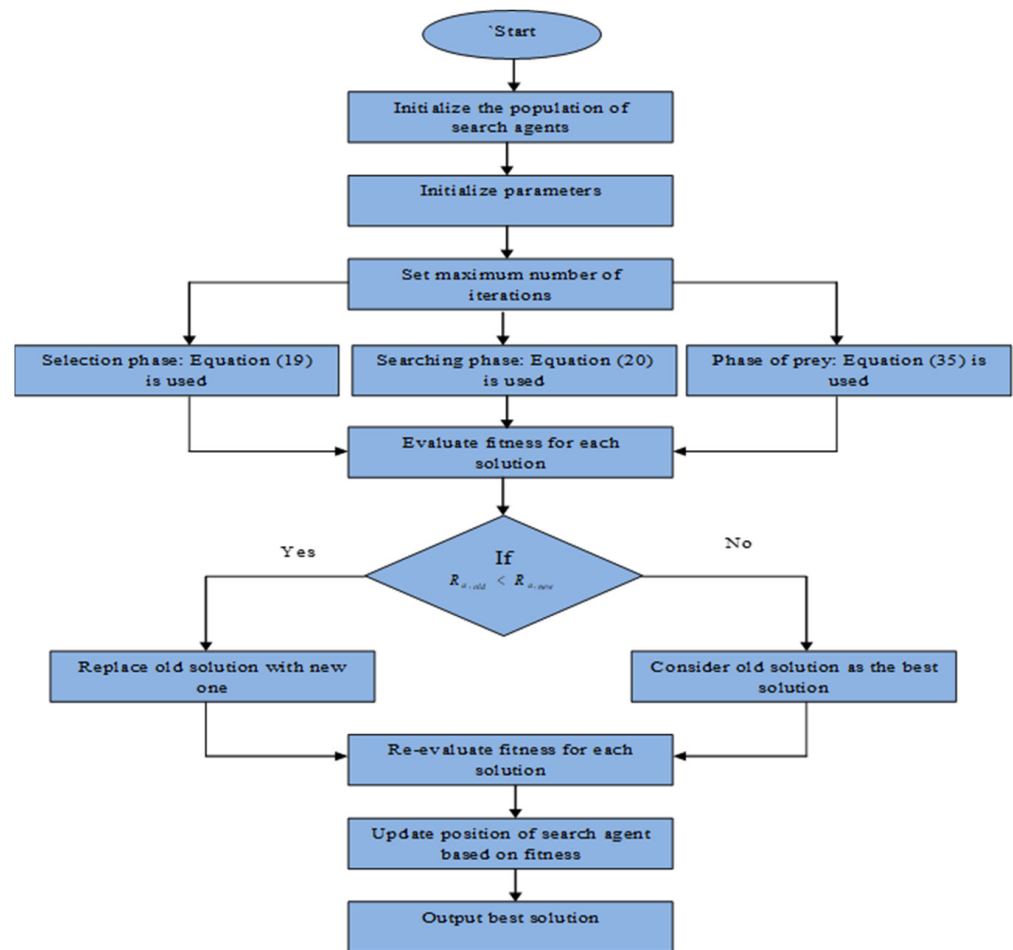
Figure 4. Flowchart of the BESSO algorithm.

Table 2 shows the notation and description of the proposed system.

Table 2. Notation and Description.

Notation	Description
M	inertia constant
Δr	deviation in rotor speed
ΔP_e	change in electrical power
ΔP_m	variation in mechanical power
D	load damping constant
ΔP_D	non-frequency sensitive load variation
$D\Delta r$	frequency sensitive load variation
$B_1 B_2$	the frequency bias coefficient
ΔP_{tie}	variation in tie-line power
Δf_1	variation in frequency corresponding to area 1
Δf_2	variation in frequency corresponding to area 2
E_a	total bald eagles in the search space
E_j	j^{th} Search agent

4. Results and Analysis

This section describes the findings obtained utilizing the BESSO-based PID controller and the comparative assessment for establishing the superiority of the proposed control strategy. The experiments were carried out using MATLAB 2021b, which was installed on a Windows 10 64-bit OS with 16GB RAM and allows for a simple and effective implementation of the proposed system.

4.1. Comparative Analysis

This section describes the comparative evaluation of the proposed BESSO-based PID based on frequency variation corresponding to area 1, frequency variation corresponding to area 2, and the variation in tie-line power.

4.2. Comparative Methods

The existing comparative methods compared with the proposed BESSO-PID strategy were PSO-PID [44,48], the Hybrid intelligent optimization-based PID controller (HIO-PID) [30,44], the Sparrow search optimization algorithm-based PID controller (SpSOA-PID) [44,47], and the Bald eagle optimization-based PID controller (BaEO-PID) [44,46].

4.3. Stability Analysis

It has been determined that the BESSO-PID is useful for controlling the frequency and regulating tie-line power. Because of this, this method was used in the proposed study to modify the controller gains for the LFC application of a two-area linked hybrid power system. The stability of the controller was assessed to determine the controller's proper settings for maintaining the dynamic operation of the system. Table 3 displays the thus-derived controller parameters. The values were 2.3922, 5.0657, 3.1965, 2.092, and 4.391 for the methods BaEO-PID, SpSOA-PID, HIO-PID, PSO-PID, and the suggested BESSO-PID, respectively. The resulting ITAE values for techniques such as the BaEO-PID, SpSOA-PID, HIO-PID, PSO-PID, and the suggested BESSO-PID are 0.0427, 0.2266, 0.7265, 1.2265, and 0.0327, respectively. Hence, from the analysis, it was evident that the BESSO-PID strategy exhibited reduced values of ITAE as compared to the conventional methods.

**Table 3.** Parameters of PID controller.

Methods	Kp1	Ki1	Kd1	Kp2	Ki2	Kd2	ITAE
BaEO-PID	10.9222	8.4322	2.7222	7.2822	8.0822	2.3922	0.0427
SpSOA-PID	10.0500	10.2565	2.4766	9.4327	8.5477	5.0657	0.2266
HIO-PID	5.5405	8.7065	5.8365	7.4885	6.4265	3.1965	0.7265
PSO-PID	8.4536	9.5233	3.0154	5.0255	7.9530	2.0920	1.2265
Proposed BESSO-PID	6.7700	8.2010	3.0231	9.0070	7.5810	4.3910	0.0327

The comparative analysis of the methods based on frequency variations corresponding to area 1, frequency variation corresponding to area 2, and the change of power in the tie-line are tabulated in Table 4. Figure 8 shows the response equivalent to Table 4. From the table, it is evident that the proposed BESSO-PID strategy obtained reduced settling time, overshoot, and undershoot under the non-linearity constraints of generation rate constraint (GRC), and governor dead band (GDB).

**Table 4.** Comparative analysis of various controllers.

Controllers	Overshoot			Settling Time (s)			Undershoot (−)		
	ΔF1	ΔF2	ΔPtie	ΔF1	ΔF2	ΔPtie	ΔF1	ΔF2	ΔPtie
PI	0.64	0.72	0.0858	30.25	30.454	25.759	-	–	-
Fuzzy [41]	0.071	0.0759	0.00357	23	23.475	27	-	-	-
PID	0.049	0.0591	0.0084	26	27	24.757	-	-	-
ANN	0.045	0.055	0.003	17.524	17	23.44	-	-	-
ANFIS	0.044	0.044	0.012	15.057	15	20.165	-	-	-
FO-PID [36]	0.0039	0.00461	0.012	7.617	8.85	18.989	0.0157	0.0143	0.00261
QOGWO-PID [22]	0.00384	0.00447	0.000786	7.624	6.789	17.32	0.0167	0.0198	0.00321
Proposed BESSO-PID	0.0001	0.0001	0	7.10	6.3656	8.5656	0.0002	0.0004	0.0007

Figure 5 shows how BESSO-PID controllers outperform conventional controllers in terms of dynamic response characteristics, such as peak overshoot, settling time, and peak undershoot related to frequency fluctuations of the two areas and power variance in tie-lines. The outcomes revealed that the BESSO-PID-based model effectively reduced overshoot, enhanced time settling, and reduced undershooting as compared with the conventional methods. The results show that the system generates a large amount of power to satisfy the rising demand for load, and that frequency oscillations were dampened by the appropriately tuned controller. In comparison to existing traditional controllers, the proposed controller swiftly returns the system to its steady state from its transitory condition. Furthermore, the controller's resilience was tested under unpredictably changing system parameters. For these adjustments, the dynamic characteristics of variation in system tie-line power and frequency were tested. The findings demonstrated that, for these uncertain modifications, the proposed controller eliminated the oscillations and promptly returned the system to its steady state.
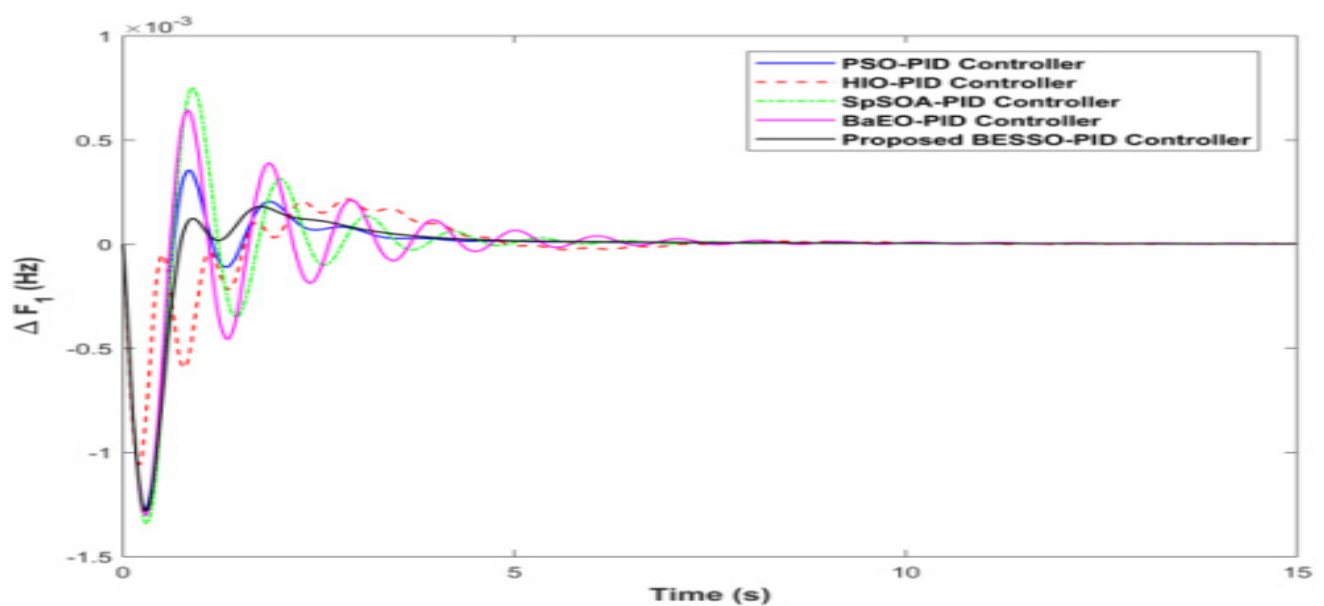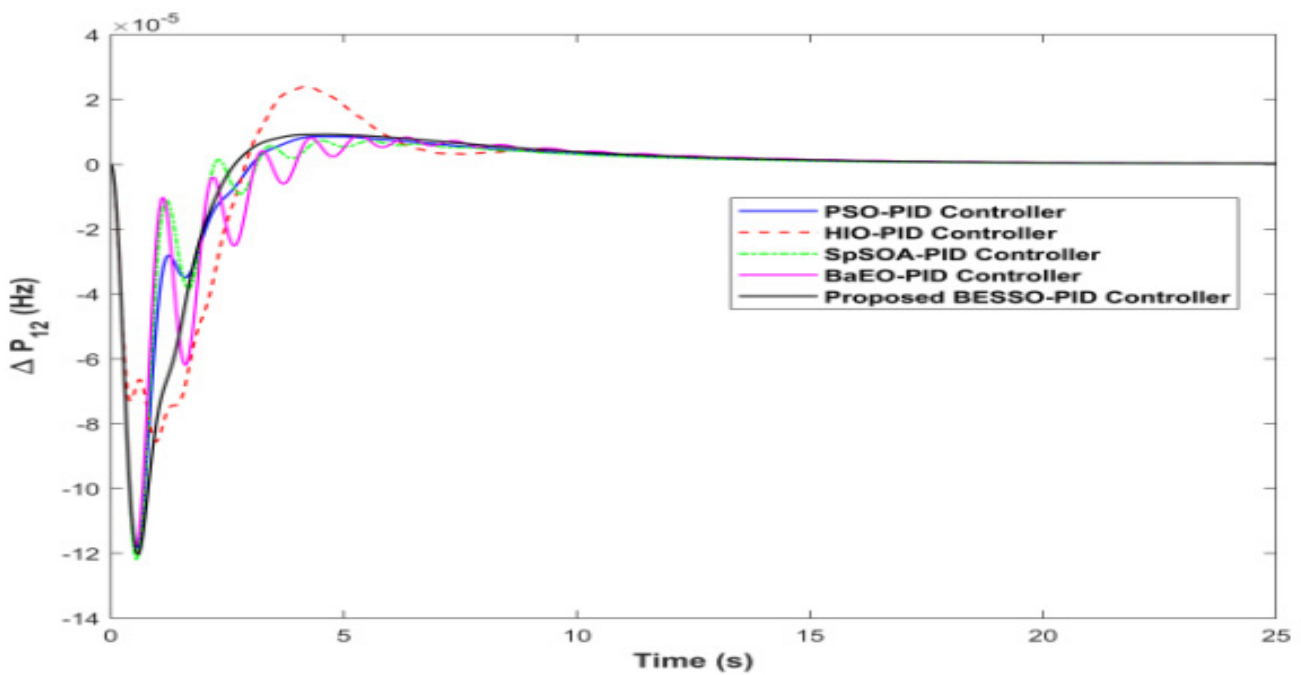

(**a**)

Figure 5. *Cont.*
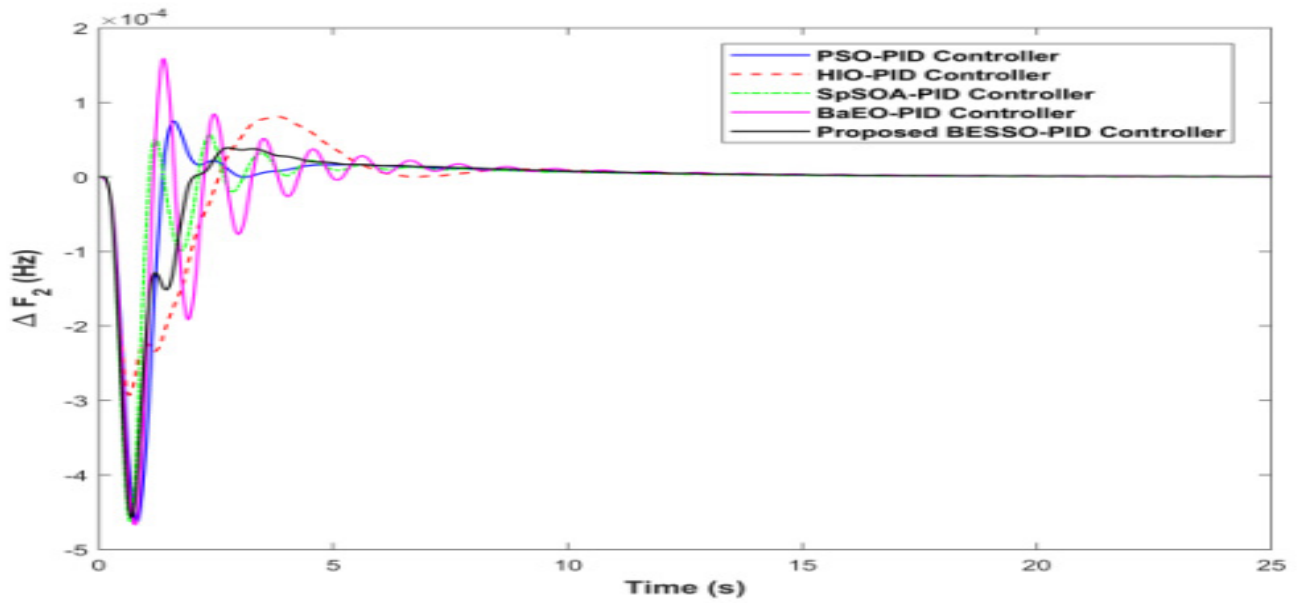
(**b**)

(**c**)

Figure 5. (**a**) Stability analysis, for change in frequency corresponding to area1. (**b**) Stability analysis, for change in frequency corresponding to area 2. (**c**) Stability analysis, for change in frequency corresponding to tie-line power.
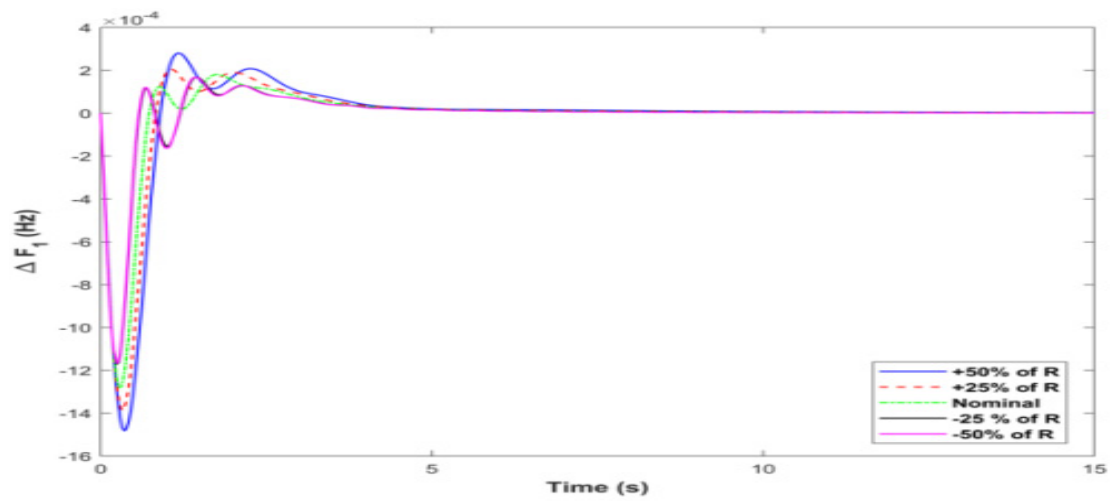
4.4. Sensitivity Analysis

This section focuses on testing the controller's resilient capabilities under the effect of substantial fluctuations in AGC system parameters. The sensitivity investigation of the BESSO-PID controller was executed in this work by adjusting the time constant of the

turbine T_t, wind turbine T_w, governor constant T_g, and droop constant R to $\hat{A} \pm 50\%$ of their nominal values while maintaining the BESSO-PID controller's optimal parameters. Table 5 shows the transient analysis based on overshoot, settling time, and undershoot as it relates to various system circumstances. Figures 6–9 show the results achieved by adjusting AGC settings throughout a range of $\hat{A} \pm 50\%$. The system parameters' transient responses are almost equal to their nominal values, representing the robustness of BESSO-PID controllers. In other words, from Figure 4, it is clear that the frequency and tie-line power remain almost similar in all the cases of variation from their nominal values. This sensitivity test indicates that re-tuning the controller settings for such significant variations in process variables from their nominal values is not necessary.

The sensitivity analysis of the BESSO-PID controller based on droop constant, turbine time constant, wind turbine variation, and governor time constant concerning change in frequency corresponding to area 1, area 2, and the change in tie-line power are described in Figures 4–7, respectively.
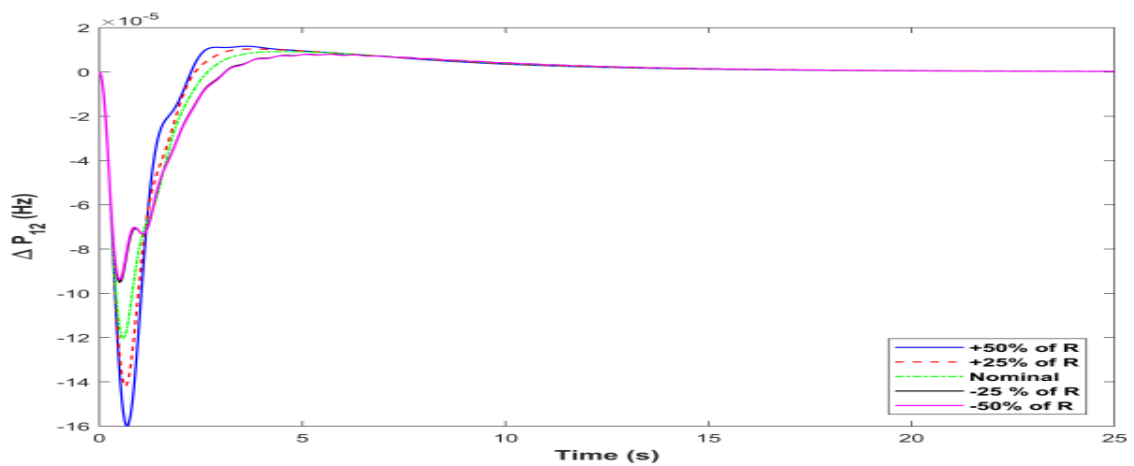
Table 5. Sensitivity analysis.

| Variation in Parameters		Settling Time (s)			Overshoot			Undershoot		
Parameter	% Variation	ΔF1	ΔF2	ΔPtie	ΔF1	ΔF2	ΔPtie	ΔF1	ΔF2	ΔPtie
	+50	9.4205	8.3761	9.1480	0.0001	0.0004	0.0006	−0.0004	−0.0006	−0.0002
	+25	6.5944	5.1545	6.0987	0.0002	0.0005	0.0007	−0.0004	−0.0006	−0.0003
R	Nominal (2.4)	0.0001	0.0001	0.0000	7.1000	8.3656	8.5656	−0.0002	−0.0004	−0.0007
	−25	14.1308	6.4432	9.1480	0.0001	0.0006	0.0006	−0.0004	−0.0004	−0.0002
	−50	14.1308	7.7318	7.9283	0.0002	0.0006	0.0009	−0.0004	−0.0004	−0.0002
	+50	10.3626	9.0205	9.7579	0.0002	0.0004	0.0009	−0.0003	−0.0005	−0.0002
	+25	10.3626	4.5102	9.1480	0.0002	0.0005	0.0005	−0.0005	−0.0006	−0.0003
Tt	Nominal (0.3)	0.0001	0.0001	0.0000	7.1000	8.3656	8.5656	−0.0002	−0.0004	−0.0007
	−25	9.4205	9.6648	10.3677	0.0001	0.0005	0.0008	−0.0004	−0.0006	−0.0002
	−50	14.1308	8.3761	10.3677	0.0002	0.0005	0.0006	−0.0004	−0.0006	−0.0002
	+50	9.4205	7.0875	7.3184	0.0002	0.0006	0.0007	−0.0005	−0.0007	−0.0002
	+25	7.5364	6.4432	9.1480	0.0002	0.0006	0.0008	−0.0004	−0.0006	−0.0003
Tw	Nominal (1)	0.0001	0.0001	0.0000	7.1000	8.3656	8.5656	−0.0002	−0.0004	−0.0007
	−25	13.1887	7.0875	6.7085	0.0002	0.0004	0.0009	−0.0004	−0.0007	−0.0002
	−50	9.4205	5.7989	6.0987	0.0002	0.0005	0.0007	−0.0005	−0.0006	−0.0003
	+50	8.4785	7.0875	9.1480	0.0002	0.0004	0.0009	−0.0004	−0.0005	−0.0002
	+25	9.4205	7.0875	8.5381	0.0002	0.0006	0.0006	−0.0006	−0.0004	−0.0003
Tg	Nominal (0.08)	0.0001	0.0001	0.0000	7.1000	8.3656	8.5656	−0.0002	−0.0004	−0.0007
	−25	6.5944	9.0205	7.9283	0.0002	0.0004	0.0008	−0.0006	−0.0006	−0.0002
	−50	7.5364	9.0205	10.3677	0.0001	0.0004	0.0008	−0.0005	−0.0007	−0.0003

(a)
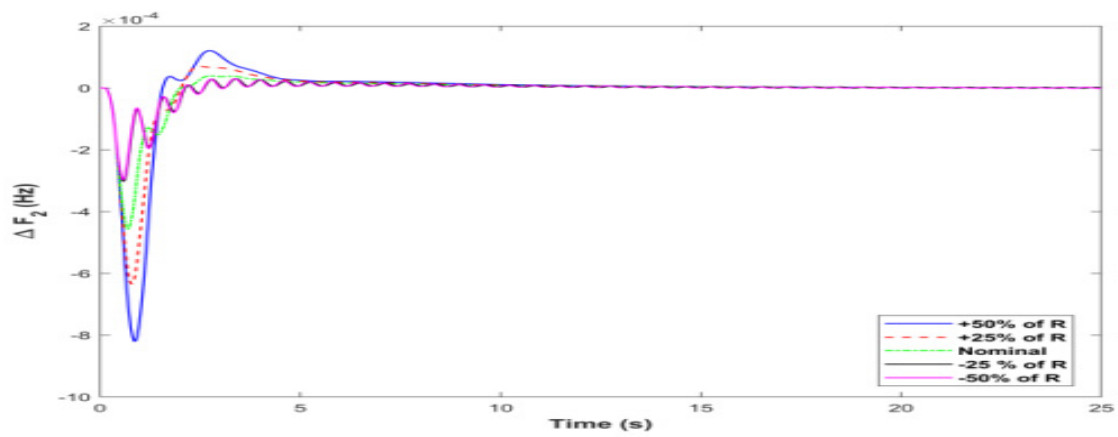
(b)

(c)

Figure 6. (**a**) Sensitivity analysis based on droop constant in terms of variation in frequency corresponding to (**a**) area 1. (**b**) Sensitivity analysis based on droop constant in terms of variation in frequency corresponding to area 2. (**c**) Sensitivity analysis based on droop constant in terms of variation in frequency corresponding to tie-line power.
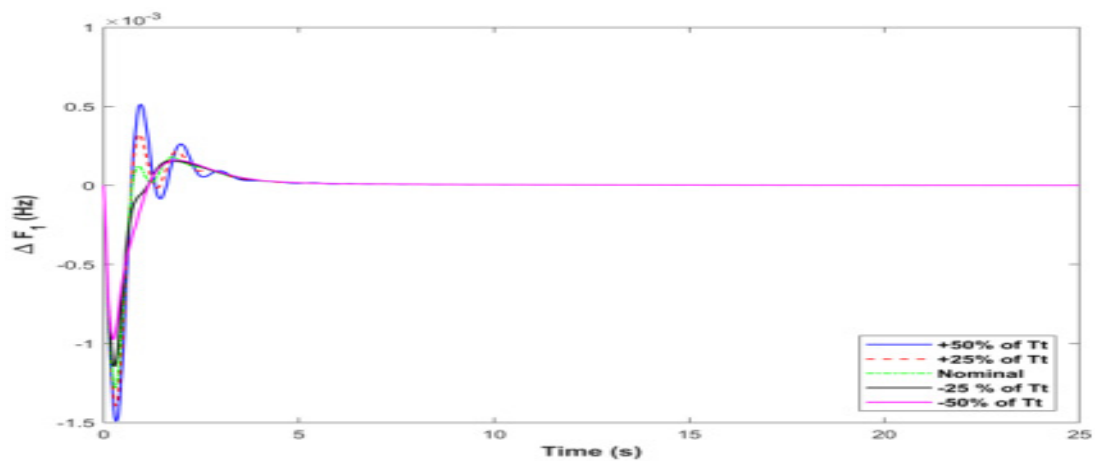
(a)
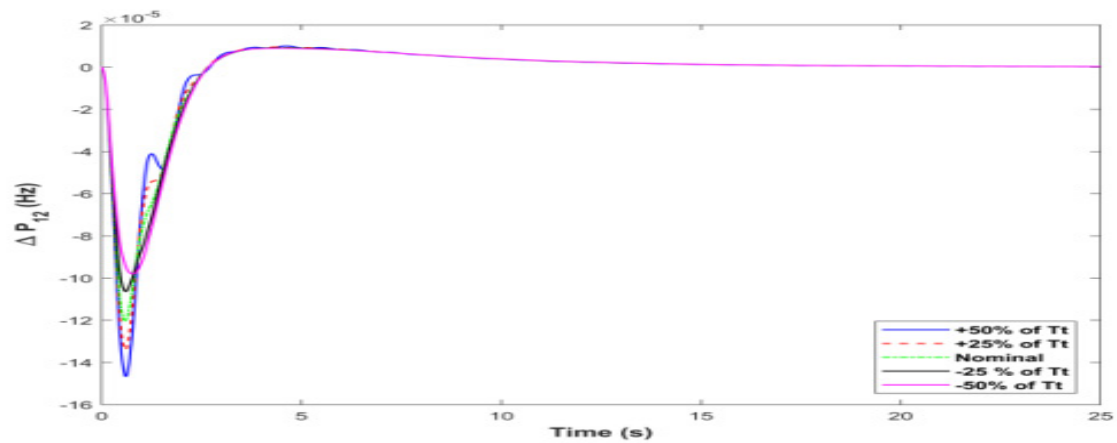
(b)
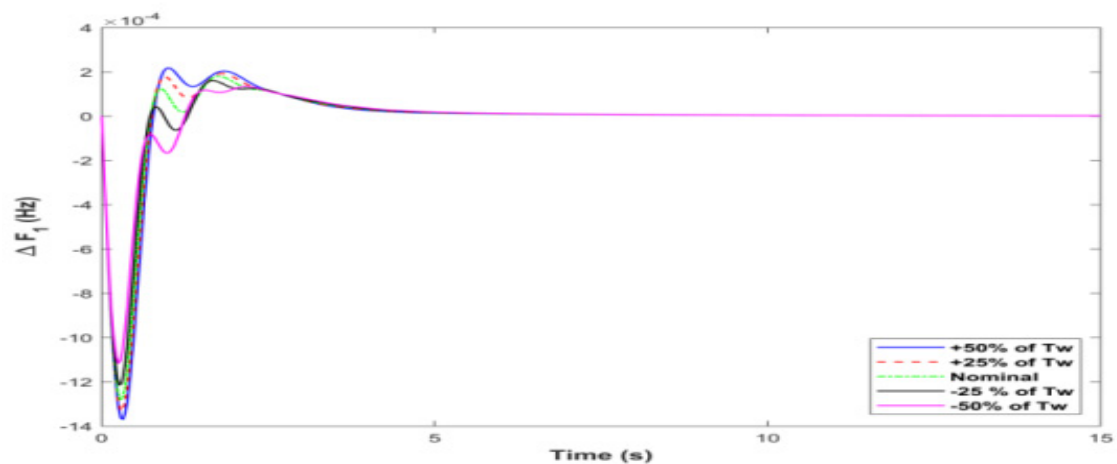
(c)

Figure 7. (**a**) Sensitivity analysis based on the Turbine Time constant of the thermal unit in terms of variation in frequency corresponding to area 1. (**b**) Sensitivity analysis based on the Turbine Time constant of the thermal unit in terms of variation in frequency corresponding to area 2. (**c**) Sensitivity analysis based on the Turbine Time constant of the thermal unit in terms of variation in frequency corresponding to tie-line power.
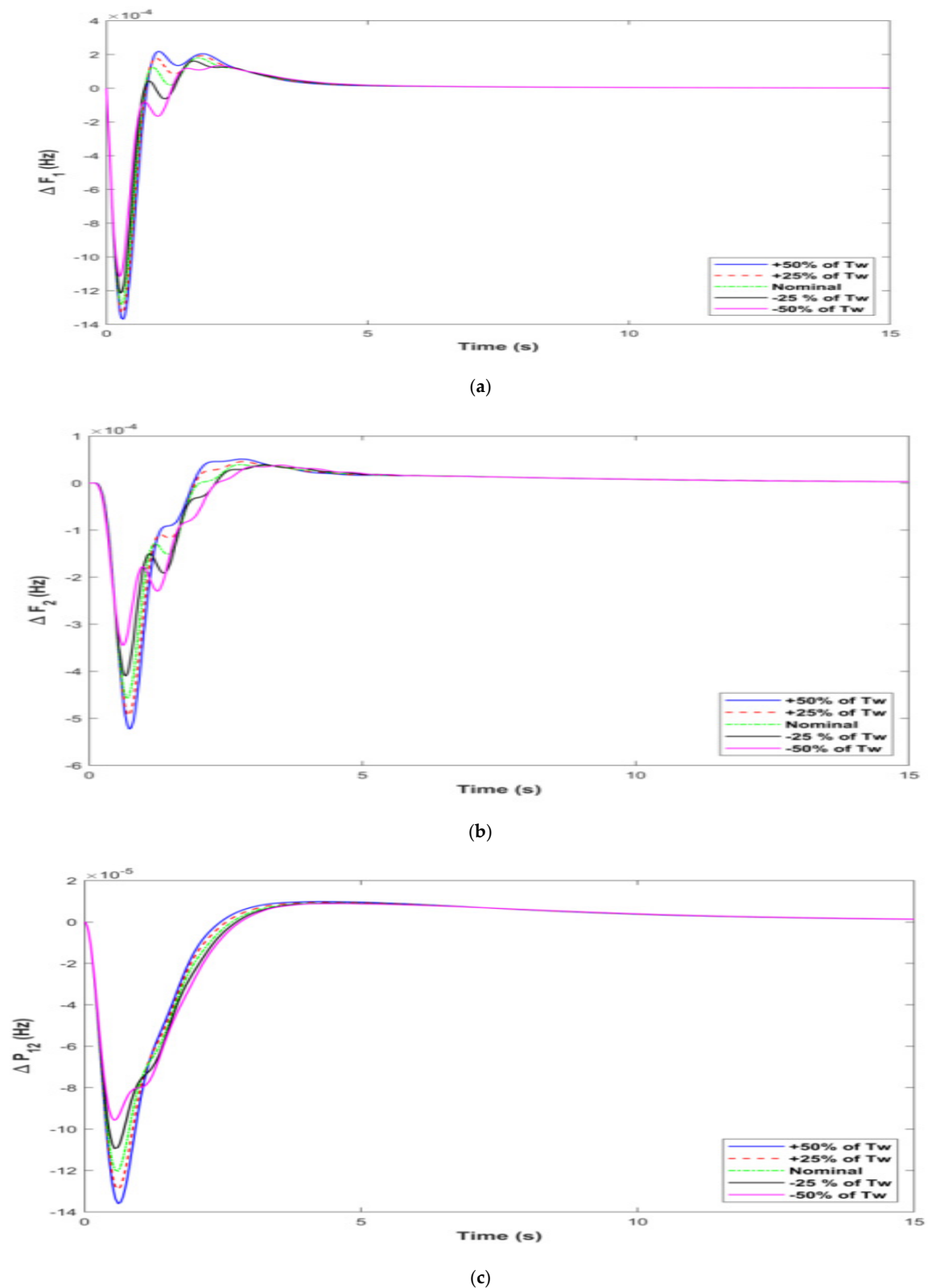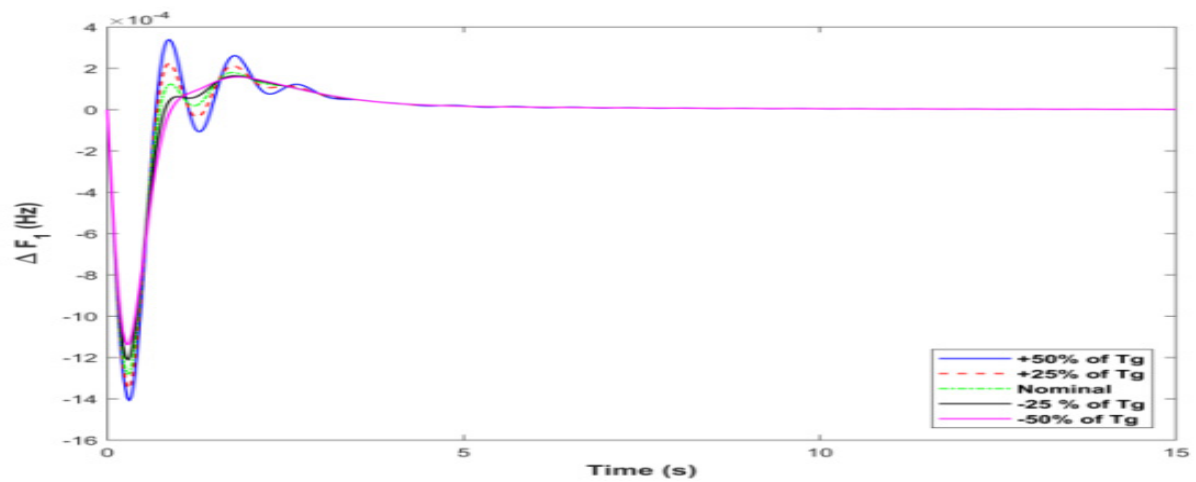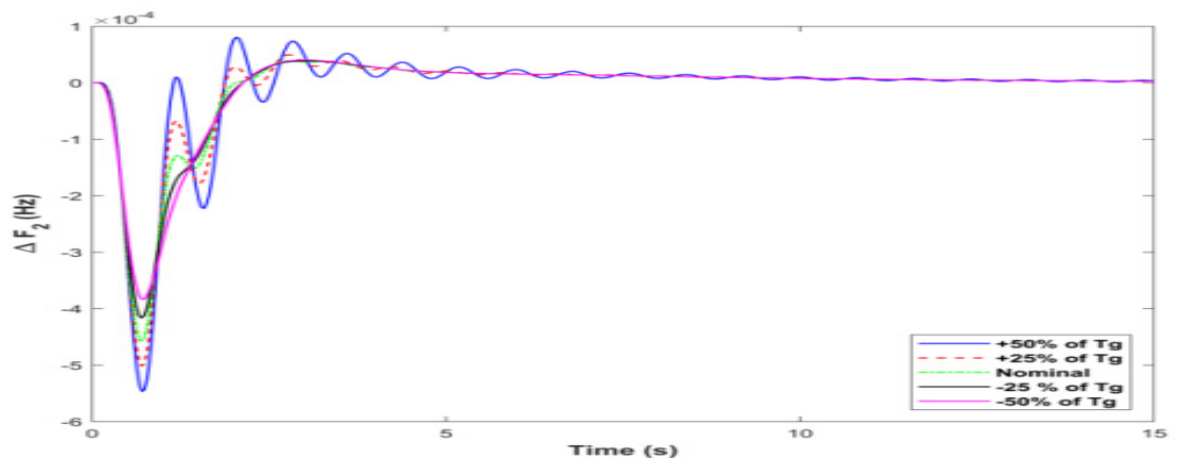
(a)

(b)

(c)

Figure 8. (**a**) Sensitivity analysis based on Wind turbine variation in terms of variation in frequency corresponding to area1. (**b**) Sensitivity analysis based on Wind turbine variation in terms of variation in frequency corresponding to area 2. (**c**) Sensitivity analysis based on Wind turbine variation in terms of variation in frequency corresponding to tie-line power.
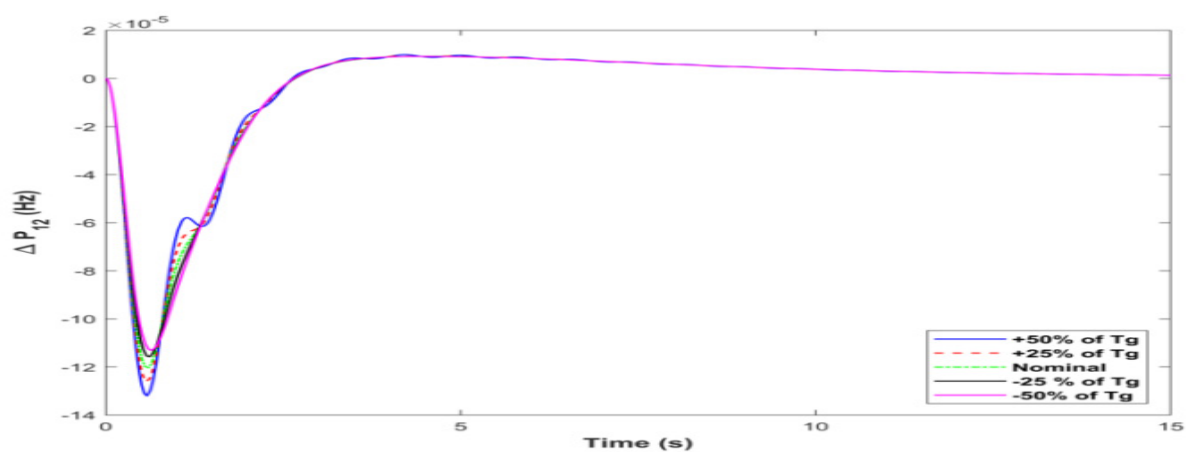
(a)

(b)

(c)

Figure 9. (**a**) Sensitivity analysis based on Governor constant analysis in terms of variation in frequency corresponding to area 1. (**b**) Sensitivity analysis based on Governor constant analysis in terms of variation in frequency corresponding to area 2. (**c**) Sensitivity analysis based on Governor constant analysis in terms of variation in frequency corresponding to tie-line power.

4.5. Sensitivity Analysis with Random Loadings

An evaluation of a mathematical model's sensitivity to its modeling assumptions is called a sensitivity analysis. How susceptible conclusions made using a specific model are to its parameters is frequently assessed in statistics. Figure 10 depicts the analysis of load patterns.
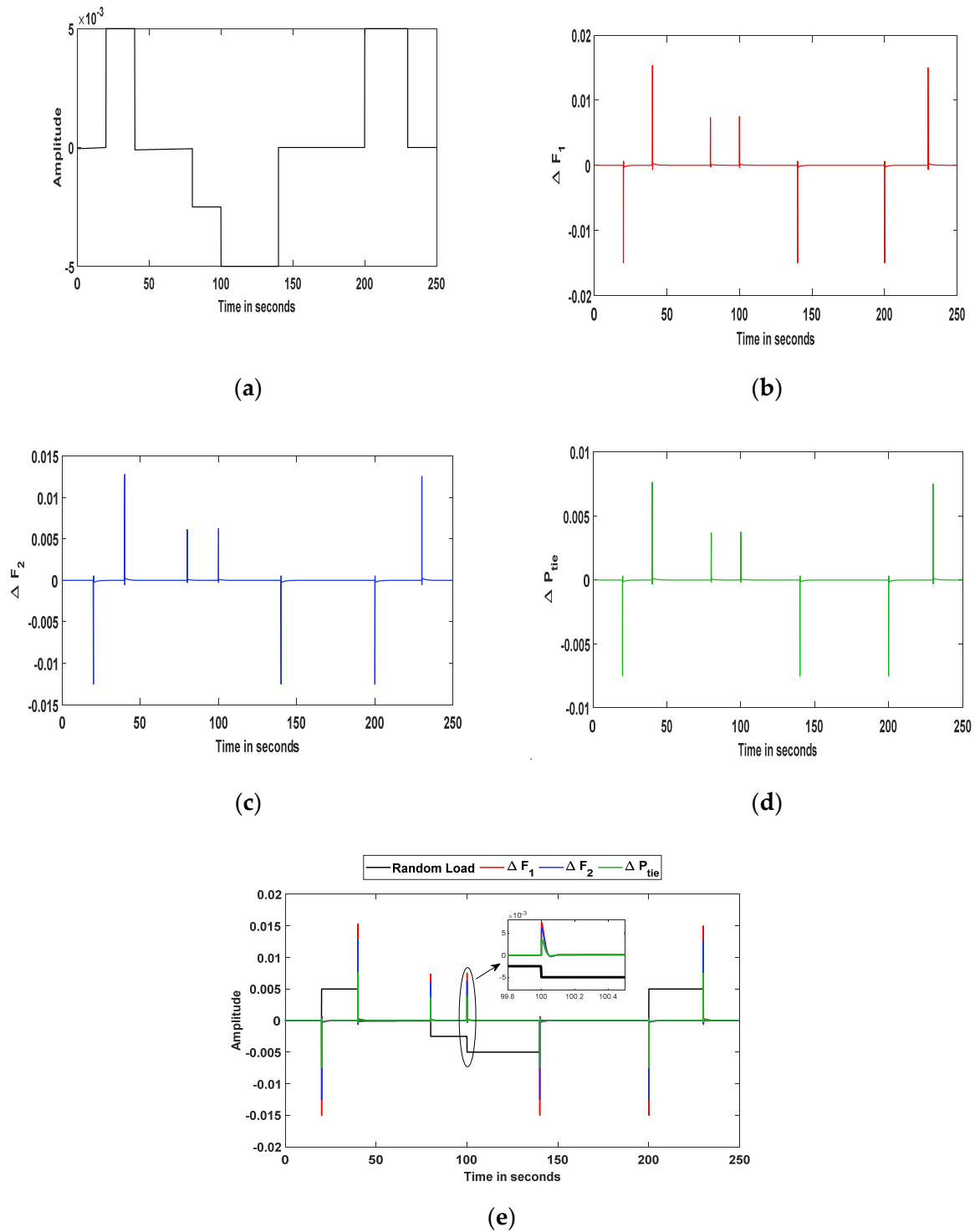

Figure 10. Analysis on random load patterns (**a**) Amplitude (**b**) area 1, (**c**) area 2, (**d**) tie-line power, and (**e**) amplitude in random load.

4.6. Computational Time Analysis

Table 6 shows the computational time analysis. The computational time of the proposed model is (~170.26) better than the existing methods, such asBaEO-PID, SpSOA-PID, HIO-PID, and PSO-PID. Thus, the superiority of the model over the other existing methods is proven.

Table 6. Analysis of Computational Time.

Methods	Time (Sec)
BaEO-PID	256.78
SpSOA-PID	250.10
HIO-PID	224.25
PSO-PID	202.23
Proposed BESSO-PID	170.26

5. Conclusions

In this paper, BESSO, a stochastic evolutionary hybrid model inspired by nature, is applied to find the best and most practical solutions to the LFC problem and tie-line power regulation in a two-area power system. In anti-predation behaviors and prey hunting, the suggested BESSO resembles the traits of sparrows and bald eagles, respectively. The optimization approach is used to fine-tune the controller settings, and the research also covers the effects of frequency measurements and nonlinearities in power systems. The findings of BESSO are compared to the results of traditional procedures to determine its efficacy. Sensitivity and stability analyses are carried out to confirm the proposed BESSO's robustness in LFC and tie-line power control. Investigations on simulated outcomes reveal that the proposed method effectively reduced the overshoot by 98%, 75%, and 100%, enhanced settling time by 32.23%, 25.72%, and 9.86%, and reduced undershoot by 97.61%, 84%, 83.72%, for ΔF_1, ΔF_2, and ΔP_{tie}, respectively, compared to the existing PSO method. In the future, the proposed idea will be tested using renewable energy sources (RES) in the presence of enhanced hybrid optimization strategies to provide improved frequency support. The suggested model's drawbacks include considerable variations in load or a large disturbance, such as a fault, for which the proposed technique is not appropriate due to the system's linear modeling. The linear design of traditional PID controllers renders them ineffective for higher-order time delay systems in the future. By using sophisticated controllers calibrated with clever meta-heuristic optimization methods, this can be avoided.

Author Contributions: Conceptualization, T.D.R. and C.K.; methodology, T.D.R. and C.K.; software, T.D.R. and C.K.; validation, P.K. and H.H.F.; formal analysis, P.K. and H.H.F.; investigation, P.K. and H.H.F.; resources, P.K. and H.H.F.; data curation, T.D.R. and C.K.; writing—original draft preparation, T.D.R. and C.K.; writing—review and editing, P.K. and H.H.F.; visualization, P.K. and H.H.F.; supervision, P.K. and H.H.F.; project administration, T.D.R. and C.K.; All authors have read and agreed to the published version of the manuscript.

Institutional Review Board Statement: Not applicable.

Informed Consent Statement: Not applicable.

Data Availability Statement: Not applicable.

Conflicts of Interest: The authors declare no conflict of interest.

References

1. Ameli, A.; Ali, H.; Ehab, F.E.; Amr, M.Y. Attack detection and identification for automatic generation control systems. *IEEE Trans. Power Syst.* **2018**, *33*, 4760–4774. [CrossRef]
2. Mohammadikia, R.; Mortaza, A. A fractional order fuzzy PID for load frequency control of four-area interconnected power system using biogeography-based optimization. *Int. Trans. Electr. Energy Syst.* **2019**, *29*, e2735. [CrossRef]
3. Kumar, R.; Sharma, V.K. Whale optimization controller for load frequency control of a two-area multi-source deregulated power system. *Int. J. Fuzzy Syst.* **2020**, *22*, 122–137. [CrossRef]
4. Shayeghi, H.; Rahnama, A.; Mohajery, R.; Bizon, N.; Mazare, A.G.; Ionescu, L.M. Multi-Area Microgrid Load-Frequency Control Using Combined Fractional and Integer Order Master–Slave Controller Considering Electric Vehicle Aggregator Effects. *Electronics* **2022**, *11*, 3440. [CrossRef]
5. Gonzalez, I.; Antonio José, C.; Francisco, J.F. IoT real time system for monitoring lithium-ion battery long-term operation in microgrids. *J. Energy Storage* **2022**, *51*, 104596. [CrossRef]
6. Coban, H.H.; Aysha, R.; Mohamed, M. Load frequency control of microgrid system by battery and pumped-hydro energy storage. *Water* **2022**, *14*, 1818. [CrossRef]
7. Shankar, R.; Pradhan, S.R.; Kalyan, C.; Rajasi, M. A comprehensive state of the art literature survey on LFC mechanism for power system. *Renew. Sustain. Energy Rev.* **2017**, *76*, 1185–1207. [CrossRef]
8. Khooban, M.; Tomislav, D.; Frede, B.; Marko, D. Shipboard microgrids: A novel approach to load frequency control. *IEEE Trans. Sustain. Energy* **2017**, *9*, 843–852. [CrossRef]
9. Mohamed, T.H.; Bevrani, H.; Hassan, A.A.; Hiyama, T. Decentralized model predictive based load frequency control in an interconnected power system. *Energy Convers.Manag.* **2011**, *52*, 1208–1214. [CrossRef]
10. Bevrani, H.; Mohammad, R.F.; Sirwan, A. Robust frequency control in an islanded microgrid: Hα and μ-synthesis approaches. *IEEE Trans. Smart Grid* **2015**, *7*, 706–717. [CrossRef]
11. Modirkhazeni, A.; Omid, N.A.; Mohammad, H.K. Improved frequency dynamic in isolated hybrid power system using an intelligent method. *Int. J. Electr. Power Energy Syst.* **2016**, *78*, 225–238. [CrossRef]
12. Khooban, M.H. Secondary load frequency control of time-delay stand-alone microgrids with electric vehicles. *IEEE Trans. Ind. Electron.* **2017**, *65*, 7416–7422. [CrossRef]
13. Singh, V.P.; Nand, K.; Paulson, S. Improved load frequency control of power system using LMI based PID approach. *J. Frankl. Inst.* **2017**, *354*, 6805–6830. [CrossRef]
14. Ali, E.S.; Sahar, M.A. Bacteria foraging optimization algorithm based load frequency controller for interconnected power system. *Int. J. Electr. Power Energy Syst.* **2011**, *33*, 633–638. [CrossRef]
15. Lu, K.; Wuneng, Z.; Guoqiang, Z.; Yiyuan, Z. Constrained population extremal optimization-based robust load frequency control of multi-area interconnected power system. *Int. J. Electr. Power Energy Syst.* **2019**, *105*, 249–271. [CrossRef]
16. Turner, G.; Jay, P.K.; Caroline, L.S.; David, A.W.; Wei-Jen, L. Design and active control of a microgrid testbed. *IEEE Trans. Smart Grid* **2014**, *6*, 73–81. [CrossRef]
17. Sahu, B.K.; Tridipta, K.P.; Jyoti, R.N.; Siddhartha, P.; Sanjeeb, K.K. A novel hybrid LUS–TLBO optimized fuzzy-PID controller for load frequency control of multi-source power system. *Int. J. Electr. Power Energy Syst.* **2016**, *74*, 58–69. [CrossRef]
18. Duman, S.; Nuran, Y.; Ismail, H.A. Load frequency control of a single area power system using Gravitational Search Algorithm. In Proceedings of the 2012 International Symposium on Innovations in Intelligent Systems and Applications, Trabzon, Turkey, 2–4 July 2012; pp. 1–5.
19. Dahab, Y.A.; Hussein, A.; Tarek, H.M. Adaptive load frequency control of power systems using electro-search optimization supported by the balloon effect. *IEEE Access* **2020**, *8*, 7408–7422. [CrossRef]
20. Ali, E.S.; Abd-Elazim, S.M. BFOA based design of PID controller for two area load frequency control with nonlinearities. *Int. J. Electr. Power Energy Syst.* **2013**, *51*, 224–231. [CrossRef]
21. Sahu, R.K.; Sidhartha, P.; Umesh, K.R.; Dillip, K.S. Teaching learning based optimization algorithm for automatic generation control of power system using 2-DOF PID controller. *Int. J. Electr. Power Energy Syst.* **2016**, *77*, 287–301. [CrossRef]
22. Guha, D.; Provas, K.R.; Subrata, B. Load frequency control of large scale power system using quasi-oppositional grey wolf optimization algorithm. *Eng. Sci. Technol. Int. J.* **2016**, *19*, 1693–1713. [CrossRef]
23. Sambariya, D.K.; Rajendra, F. A novel Elephant Herding Optimization based PID controller design for Load frequency control in power system. In Proceedings of the 2017 International Conference on Computer, Communications and Electronics (Comptelix), Jaipur, India, 1–2 July 2017; pp. 595–600.
24. Alayi, R.; Zishan, F.; Seyednouri, S.R.; Kumar, R.; Ahmadi, M.H.; Sharifpur, M. Optimal load frequency control of island microgrids via a PID controller in the presence of wind turbine and PV. *Sustainability* **2021**, *13*, 10728. [CrossRef]
25. Guha, D.; Provas, K.R.; Subrata, B. Whale optimization algorithm applied to load frequency control of a mixed power system considering nonlinearities and PLL dynamics. *Energy Syst.* **2020**, *11*, 699–728. [CrossRef]
26. Guha, D.; Provas, K.R.; Subrata, B. Maiden application of SSA-optimised CC-TID controller for load frequency control of power systems. *IET Gener.Transm. Distrib.* **2019**, *13*, 1110–1120. [CrossRef]
27. Barakat, M.; Ahmed, D.; Hesham, F.H.; Gerges, M.S. Controller parameters tuning of water cycle algorithm and its application to load frequency control of multi-area power systems using TD-TI cascade control. *Evol. Syst.* **2022**, *13*, 117–132. [CrossRef]

28. Arora, K.; Ashok, K.; Vikram, K.K.; Deepak, P.; Sudan, J.; Bhanu, S.; Gyanendra, P.J. Optimization methodologies and testing on standard benchmark functions of load frequency control for interconnected multi area power system in smart grids. *Mathematics* **2020**, *8*, 980. [CrossRef]

29. Wang, N.; Jing, Z.; Yu, H.; Min, L.; Ying, Z.; Chaokuan, C.; Yerui, G.; Yongheng, R. Load-frequency control of multi-area power system based on the improved weighted fruit fly optimization algorithm. *Energies* **2020**, *23*, 437. [CrossRef]

30. Gupta, D.K.; Amitkumar, V.J.; Bhargav, A.; Avireni, S.; Nicu, B.; Phatiphat, T. Load Frequency Control Using Hybrid Intelligent Optimization Technique for Multi-Source Power Systems. *Energies* **2021**, *6*, 1581. [CrossRef]

31. Tripathy, D.; Barik, A.K.; Choudhury, N.B.D.; Sahu, B.K. Performance comparison of SMO-based fuzzy PID controller for load frequency control. In *Soft Computing for Problem Solving*; Springer: Singapore, 2019; pp. 879–892.

32. Shafei, M.A.R.; Doaa, K.I.; Mostafa, B. Application of PSO tuned fuzzy logic controller for LFC of two-area power system with redox flow battery and PV solar park. *Ain Shams Eng. J.* **2022**, *13*, 101710. [CrossRef]

33. Ali, T.; Malik, S.A.; Daraz, A.; Aslam, S.; Alkhalifah, T. Dandelion Optimizer-Based Combined Automatic Voltage Regulation and Load Frequency Control in a Multi-Area, Multi-Source Interconnected Power System with Nonlinearities. *Energies* **2022**, *15*, 8499. [CrossRef]

34. Kumar, A.; Gupta, D.K.; Ghatak, S.R.; Appasani, B.; Bizon, N.; Thounthong, P. A Novel Improved GSA-BPSO Driven PID Controller for Load Frequency Control of Multi-Source Deregulated Power System. *Mathematics* **2022**, *10*, 3255. [CrossRef]

35. Padhy, S.; Siddhartha, P. A hybrid stochastic fractal search and pattern search technique based cascade PI-PD controller for automatic generation control of multi-source power systems in presence of plug in electric vehicles. *CAAI Trans.Intell. Tech.* **2017**, *2*, 12–25. [CrossRef]

36. Morsali, J.; Kazem, Z.; Mehrdad, T.H. Applying fractional order PID to design TCSC-based damping controller in coordination with automatic generation control of interconnected multi-source power system. *Eng. Sci. Tech. Int. J.* **2017**, *20*, 1–17. [CrossRef]

37. Ma, M.; Chunyu, Z.; Xiangjie, L.; Hong, C. Distributed model predictive load frequency control of the multi-area power system after deregulation. *IEEE Trans. Ind. Electron.* **2016**, *64*, 5129–5139. [CrossRef]

38. Lal, D.K.; Ajit, K.B.; Tripathy, M. Load frequency control of multi area interconnected microgrid power system using grasshopper optimization algorithm optimized fuzzy PID controller. In Proceedings of the 2018 Recent Advances on Engineering, Technology and Computational Sciences (RAETCS), Allahabad, India, 6–8 February 2018; pp. 1–6.

39. Garcia-Gracia, M.; Comech, M.P.; Sallan, J.; Llombart, A. Modelling wind farms for grid disturbance studies. *Renew. Energy* **2008**, *9*, 2109–2121. [CrossRef]

40. Kosterev, D. Hydro turbine-governor model validation in pacific northwest. *IEEE Trans. Power Syst.* **2004**, *8*, 1144–1149. [CrossRef]

41. Kouba, N.E.Y.; Menaa, M.; Hasni, M.; Boudour, M. Load frequency control in multi-area power system based on fuzzy logic-PID controller. In Proceedings of the 2015 IEEE International Conference on Smart Energy Grid Engineering (SEGE), Oshawa, ON, Canada, 17–19 August 2015; pp. 1–6.

42. Khanjanzadeh, A.; Soodabeh, S.; Babak, M.; Mahmud, F. Integrated multi-area power system with HVDC tie-line to enhance load frequency control and automatic generation control. *Electr. Eng.* **2020**, *11*, 1223–1239. [CrossRef]

43. Pourmousavi, S.A.; Hashem, N.M. Introducing dynamic demand response in the LFC model. *IEEE Trans. Power Syst.* **2014**, *29*, 1562–1572. [CrossRef]

44. Kouba, N.; Mohamed, M.; Mourad, H.; Mohamed, B. LFC enhancement concerning large wind power integration using new optimised PID controller and RFBs. *IET Gener.Transm. Distrib.* **2016**, *10*, 4065–4077. [CrossRef]

45. Farook, S.; Sangameswara, R.P. AGC controllers to optimize LFC regulation in deregulated power system. *Int. J. Adv. Eng. Tech.* **2011**, *10*, 278.

46. Alsattar, H.A.; Zaidan, A.A.; Zaidan, B.B. Novel meta-heuristic bald eagle search optimisation algorithm. *Artif.Intell. Rev.* **2020**, *53*, 2237–2264. [CrossRef]

47. Xue, J.; Bo, S. A novel swarm intelligence optimization approach: Sparrow search algorithm. *Syst. Sci.Control Eng.* **2020**, *8*, 22–34. [CrossRef]

48. Daraz, A.; Suheel, A.M.; Athar, W.; Ahmad, T.A.; Ihsan, U.; Zahid, U.; Sheraz, A. Automatic Generation Control of Multi-Source Interconnected Power System Using FOI-TD Controller. *Energies* **2021**, *14*, 5867. [CrossRef]